Carbohydrate Polymers 86 (2011) 1281–1290

Contents lists available at ScienceDirect

Carbohydrate Polymers

journal homepage: www.elsevier.com/locate/carbpol

Interactions of structurally different hemicelluloses with nanofibrillar cellulose

Paula Eronen[a], Monika Österberg[a,*], Susanna Heikkinen[b], Maija Tenkanen[b], Janne Laine[a]

[a] Department of Forest Products Technology, School of Chemical Technology, Aalto University, P.O. Box 16300, FI-0076 Aalto, Finland
[b] Department of Food and Environmental Sciences, University of Helsinki, P.O. Box 27, FI-00014 University of Helsinki, Finland

ARTICLE INFO

Article history:
Received 23 April 2011
Received in revised form 31 May 2011
Accepted 13 June 2011
Available online 12 July 2011

Keywords:
NFC
Arabinoxylan
Galactoglucomannan
Quartz crystal microbalance
Hardwood
Softwood

ABSTRACT

Both cellulose nanofibrils and hemicelluloses are promising renewable alternatives for sustainable composite materials. Nanofibrils can enhance the material properties and modified hemicelluloses can be used to functionalize nanofibrillar cellulose. For optimum performance the interactions between the components have to be known. In this work the interactions between cellulose nanofibrils prepared from hardwood and softwood kraft pulps without chemical or enzymatic modification and well characterized hemicelluloses from different origins were studied. The sorption and the layer properties were quantified in the aqueous state using quartz crystal microbalance with dissipation (QCM-D). The results verified that hemicelluloses have a natural affinity towards cellulose nanofibrillar substrates. Comparison of nanofibrils prepared from hardwood and softwood kraft pulp reveal that the different hemicellulose concentration and composition of the nanofibrillar cellulose affects the adsorption of hemicelluloses. However, the hemicellulose structure affected the adsorbed layers even more significantly than the origin of the cellulose nanofibrils.

1. Introduction

The increasing interest in bioeconomy and sustainable materials is leading towards more efficient exploitation of the plant kingdom. Various abundantly available plant fibres and cell wall polysaccharides, such as cellulose microfibril structures and hemicelluloses have envisaged potential as renewable raw-materials in several future applications (Ebringerová, 2005; Eichhorn et al., 2010; Hansen & Plackett, 2008). In plant cell walls hemicelluloses interact with cellulose microfibrils and lignin thus forming the unique natural nanocomposite structure (Fengel & Wegener, 1984; Scheller & Ulvskov, 2010). Botanical origin and cytological localization are the main factors influencing the hemicellulose composition and relative amount in the plant cell wall (Joseleau, Comtat, & Ruel, 1992; Sjöström, 1993). Hemicelluloses in angiosperms (monocots such as grasses and cereals and dicots such as hardwoods) are mainly xylans whereas in gymnosperms (such as softwoods) the main hemicelluloses are glucomannans in addition to some xylans. Thus, composition of hemicelluloses varies notably between softwoods and hardwoods, and influences properties throughout the wood end products (Sjöström, 1993).

Galactoglucomannans in softwoods are composed of a backbone with (1 → 4)-linked β-D-mannopyranosyl and β-D-glucopyranosyl units substituted with (1 → 6)-linked α-D-galactopyranosyl and acetyl groups (Fig. 1). They are located mainly in the secondary cell wall where they form tight and strong associations with highly ordered cellulose microfibrils (Salmén & Olsson, 1998; Scheller & Ulvskov, 2010; Whitney, Brigham, Darke, Reid, & Gidley, 1998). All xylans are built up of (1 → 4)-linked β-D-xylopyranosyl backbone. In dicots, xylans are further substituted with (1 → 2)-linked 4-*O*-methyl-α-D-glucopyranosyl uronic acid and acetyl groups (glucuronoxylans) whereas (1 → 3)- and/or (1 → 2)-linked α-L-arabinofuranosyl units are the main substituents in monocot xylans (arabinoxylans) (Fig. 1). Xylans in softwoods carry both (1 → 3)-linked α-L-arabinofuranosyl and (1 → 2)-linked 4-*O*-methyl-α-D-glucopyranosyl uronic acid substituents (arabinoglucuronoxylans). Xylans are also associated with cellulose microfibrils in the secondary cell wall but have slightly different stereochemistry compared to β-glucan and β-mannan structures. Instead of mannan's 2-fold structure, xylan's backbone has a 3-fold screw-structure, caused by the absence of a primary hydroxyl group at C(6). This may enhance the hydrophobic interactions of xylans with lignin (Almond & Sheehan, 2003; Joseleau et al., 1992; Picout, Ross-Murphy, Errington, & Harding, 2003; Salmén & Olsson, 1998). Interactions of hardwood-extracted xylan with various cellulose substrates have been studied (Linder, Bergman, Bodin, & Gatenholm, 2003; Paananen et al., 2004; Westbye, Svanberg, & Gatenholm, 2006), but due to the low water solubility of the alkaline

* Corresponding author. Tel.: +358 50 5497218; fax: +358 9 47024259.
E-mail addresses: paula.eronen@aalto.fi (P. Eronen), monika.osterberg@aalto.fi (M. Österberg), susanna.L.heikkinen@helsinki.fi (S. Heikkinen), maija.tenkanen@helsinki.fi (M. Tenkanen), janne.laine@aalto.fi (J. Laine).

0144-8617/$ – see front matter © 2011 Elsevier Ltd. All rights reserved.
doi:10.1016/j.carbpol.2011.06.031

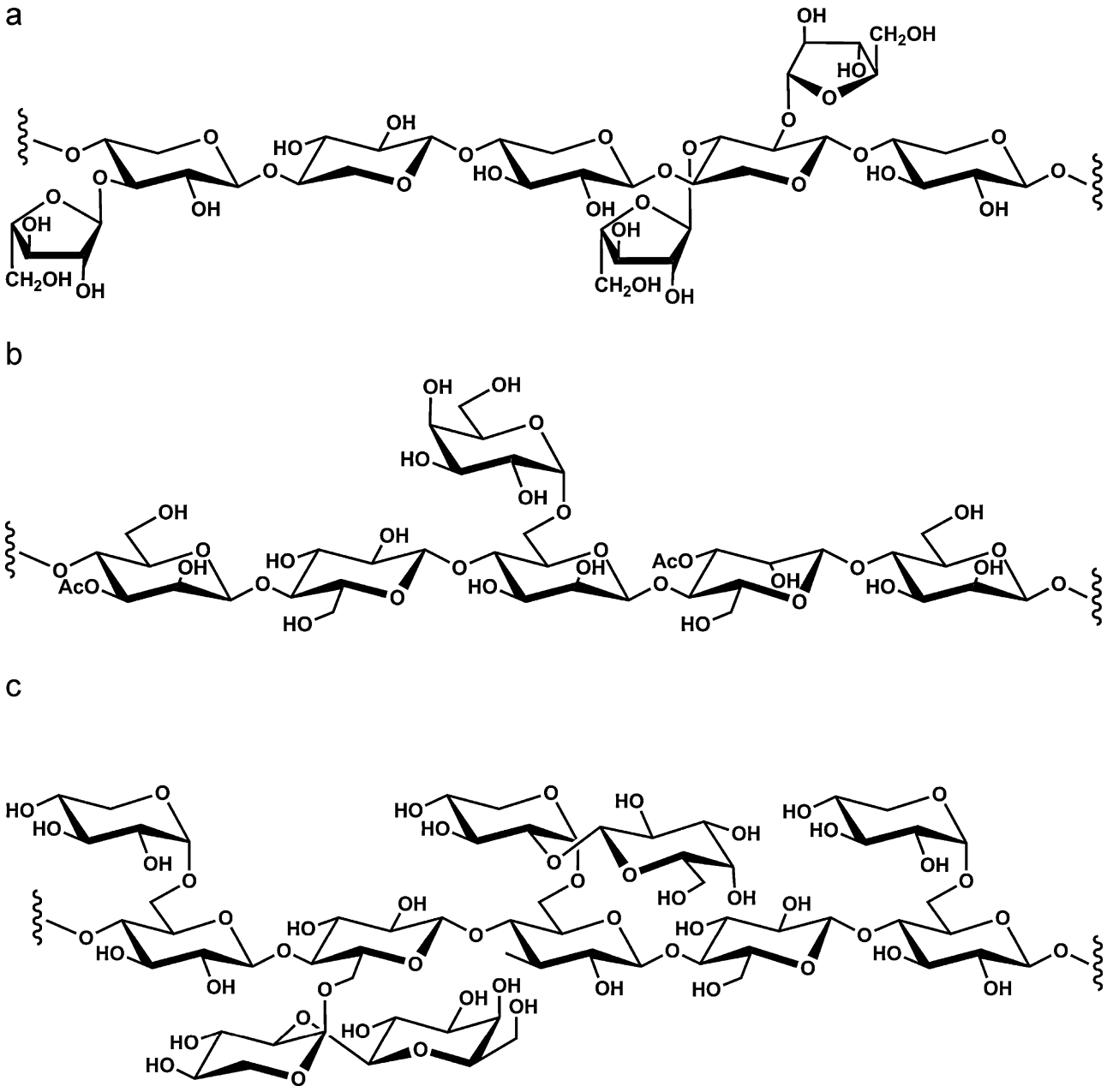

Fig. 1. Schematic chemical structures of (a) wheat arabinoxylan, (b) spruce galactoglucomannan, and (c) xyloglucan from tamarind seed.

extracted hardwood xylans (acetyl groups are lost in alkaline conditions), the interactions have somewhat been governed by the self-aggregation of xylans. Xyloglucans are particularly present in the growing primary cell walls of dicots. They are composed of a (1 → 4)-linked β-D-glucopyranosyl backbone with (1 → 6)-linked α-D-xylopyranosyl side groups which further may carry (1 → 2)-linked β-D-galactopyranosyl units (Fig. 1). Xyloglucans have a very strong ability to interact with cellulose (Burton, Gidley, & Fincher, 2010) and are expected to bring flexibility via crosslinking the spaces between crystalline microfibrils (Whitney et al., 1998; Zhou, Rutland, Teeri, & Brumer, 2007).

Micro- or nanofibrillar cellulose (MFC or NFC) is emerging as a highly potential new wood-derived material. NFC consists of fibrils liberated from the cell wall structure to much smaller dimensions than that of traditional pulp fibres (Siró & Plackett, 2010). The advantages of these extra small fibrils include their flexibility and high aspect ratio (Pääkkö et al., 2007). Without chemical modification, ultrathin films of NFC retain the chemical composition and fibrillar morphology of the original pulp fibres (Ahola, Salmi, Johansson, Laine, & Österberg, 2008). However, it is not clear what happens to the hemicelluloses present in raw pulp materials during the extreme disintegration process. Hemicelluloses inhibit the coalescence of cellulose microfibrils and thus improve fibrillation into nanosized fibrils (Iwamoto, Abe, & Yano, 2008) and pulp beatability (Lima, Oliveira, & Buckeridge, 2003). Kraft cooking causes xylans to redistribute and readsorb on fibre surfaces (Yllner & Enström, 1957), resulting in a notably higher concentration of xylan on the fibre surface compared to inner layers (Dahlman, Jacobs, & Sjöberg, 2003). However, it is not known exactly how xylan is assembled in the NFC gel nor how it is distributed in ultrathin NFC films where the NFC gel is further fractioned, diluted and, e.g. spin-coated on a solid substrate (Ahola, Myllytie, Österberg, Teerinen, & Laine, 2008; Ahola, Salmi, et al., 2008). Even the most surface sensitive chemical spectroscopy techniques have limitations in precisely

Table 1
Monosaccharide composition (%) and molecular weight of polysaccharides studied.

Sample	Abbrev.	Ara	Xyl	Glc	Gal	Man	M_w (kDa) (DMSO)	M_w (kDa) (H_2O)	Reference
Oat spelt arabinoxylan	OAX	12	83	5			58[a]	nd	Mikkonen et al. (2009)
Wheat arabinoxylan	WAX	31	61	8			319	336	Virkki et al. (2008) and Pitkänen et al. (2009)
Enzymatically treated WAX	WAX_e	33[a]	59[a]	8[a]			76[a]	89[a]	
Rye arabinoxylan	RAX	33	66	1			246	289	Höije et al. (2008), and Pitkänen et al. (2009)
Spruce galactoglucomannan	GGM	3.4	1.4	18	13	58	23[a]	60	Xu et al. (2007)
Xyloglucan	XG		36	48	16		nd	470	Parikka et al. (2010)

nd, not determined.
[a] This study.

distinguishing the chemical composition of the carbohydrate structures at the nanometer scale.

The aim of this work was to study the non-ionic interactions of promising biomaterials, hemicelluloses and cellulose nanofibrils. Hemicelluloses chosen have potential to be isolated from currently discarded by-products. Galactoglucomannans could be collected from thermomechanical pulping (TMP) process waters (Willför, Sundberg, Tenkanen, & Holmbom, 2008) and arabinoxylans extracted from leftover agricultural waste. Furthermore, cereal-derived arabinoxylans are envisaged products from future agro-biorefineries. A systematic comparison of NFC substrates prepared from different raw materials was done to improve the knowledge of fibre cellulose interactions with hemicelluloses. Here we have found that the side-group substitution pattern of arabinoxylans could be correlated with the adsorbed layer structure. The chemical composition of NFC raw material also influenced the conformation of the adsorbed hemicelluloses, indicating a tight association with mannan-containing components. In addition to the increased fundamental understanding of the interactions between hemicelluloses and cellulose in native wood, these findings are also valuable when tailoring hemicelluloses or other polysaccharides to be used for NFC functionalization/modification for new applications. While it is easy to chemically modify hemicelluloses, this study indicates what structural aspects are important to achieve high adsorption on NFC.

2. Materials and methods

2.1. Nanocellulose substrates

The nanofibrillar cellulose (NFC), obtained from The Finnish Centre for Nanocellulosic Technologies, was specially prepared for model film studies. The starting material was either never-dried bleached kraft birch or spruce pulp from a Finnish pulp mill. The birch pulp was treated with numerous passes (~30) through a high-pressure fluidizer (Microfluidics, M-110Y) to disintegrate the fibre structure into fibrils. Except for fewer passes (~15) through the fluidizer, the spruce pulp was prepared the same way. The consistencies for birch- and spruce nanofibrillated cellulose gels were ca 1.6 and 1.2%, respectively. The carbohydrate composition for original pulp and the resulting NFC gels were very similar. Hardwood pulp/NFC had a composition of 73% glucose, 26% xylose and 1% mannose, whereas softwood pulp/NFC consisted of 84% glucose, 9% xylose, 6% mannose, 0.6% arabinose and 0.2% galactose (Tenkanen et al., 1999). A procedure developed by Ahola, Salmi, et al. (2008) was followed to remove the aggregated fibril bundles and to prepare ultrathin films from only the nanosized fraction (consistency of about 1.2 g/l as determined gravimetrically). Either silica coated quartz crystal microbalance with dissipation QCM-D (QSX303, Q-Sense AB, Västra Frölunda, Sweden) or gold coated surface plasmon resonance SPR (Biacore SIA Au-kit, GE Healthcare, Uppsala, Sweden) sensors were used as substrates. In contrast to Ahola, Salmi, et al. (2008) cationic polyethylene imine (PEI, Polysciences Inc., M_w 50–100,000, diluted at 1 mg/ml) was used as the anchoring agent to facilitate nanofibril attachment on the substrates, using self-assembly for QCM-D sensors or spin-coating for SPR sensors (1 min, 3000 rpm). Fresh films were prepared 24 h prior to measurements and stabilized overnight in water to exclude the effects of swelling.

2.2. Polysaccharides

High molecular weight (M_w), high viscosity arabinoxylans from rye and wheat flours (RAX and WAX, respectively) and xyloglucan (XG) from tamarind seed were purchased from Megazyme (Ireland). Oat-spelt arabinoxylan (OAX) was obtained from Sigma–Aldrich (X0627, Germany) and was treated before use according to Mikkonen et al. (2009) to remove most of the insoluble material. O-acetyl galactoglucomannan (GGM) was collected from the industrial process waters of Finnish pulp mill by a previously developed method (Willför, Rehn, Sundberg, Sundberg, & Holmbom, 2003) and further purified as described by Mikkonen et al. (2010). WAX sample with low M_w was prepared by enzymatic hydrolysis with Shearzyme (endo-1,4-β-D-xylanase, 49,100 nkat/ml, Novozymes, Denmark). WAX sample (10 g/l) in 25 mM sodium acetate buffer, pH 5.0, was incubated with a xylanase dosage of 100 nkat/g of WAX, at +40 °C for 2 h. The enzyme reaction was terminated by keeping the sample in the boiling water bath for 10 min after which the sample was dialyzed (MWCO 12–14,000 Da) against water and freeze dried.

The carbohydrate composition, and molar mass and solution properties of most of the polysaccharides used have previously been characterized extensively (Höije, Sternemalm, Heikkinen, Tenkanen, & Gatenholm, 2008; Mikkonen et al., 2009; Parikka et al., 2010; Pitkänen, Virkki, Tenkanen, & Tuomainen, 2009; Virkki, Maina, Johansson, & Tenkanen, 2008; Xu, Willför, Sundberg, Petterson, & Holmbom, 2007) and some of the main properties are summarized in Table 1 and the chemical structures are presented in Fig. 1. Molar mass of OAX, GGM, and enzymatically hydrolyzed WAX (WAX_e) was determined by high performance size exclusion chromatography (HPSEC) in DMSO eluent containing 0.01 M LiBr and in aqueous 0.1 M $NaNO_3$ eluent according to the method described previously (Pitkänen et al., 2009). Monosaccharide composition of WAX_e was determined by degrading the polymer to monomers by acid methanolysis after which the monosaccharides were analysed as their trimethylsilyl derivatives by GC-FID (Sundberg, Sundberg, Lillandt, & Holmbom, 1996). L(+)-Arabinose, D(+)xylose, and D(+)-glucose (Merck, Darmstadt, Germany) were used as standards. Polysaccharides were diluted to concentration of 100 mg/l with extra-purified deionized water (Millipore synergy UV, Millipore, S.A.S, Molsheim, France).

2.3. Quartz crystal microbalance with dissipation (QCM-D)

The in situ attachment of hemicelluloses to nanofibrillar cellulose films was monitored with a QCM-D instrument (Q-Sense E4,

Q-Sense Västra Frölunda, Sweden) based on oscillation changes of a piezoelectric quartz sensor. When material adsorbs on the surface, the oscillation frequency decreases and the change from the fundamental frequency (5 MHz) and its several overtones is detected (Rodahl, Höök, Krozer, Brzezinski, & Kasemo, 1995). The adsorbed mass per unit surface is proportional to the decrease in the resonance frequency and can be estimated via the Sauerbrey equation,

$$\Delta m = -\frac{C\Delta f}{n}, \quad (1)$$

where C is the sensitivity constant (in our instrument $C = 0.177\,\mathrm{mg/m^2}$) and n (=3) is the overtone number. However, it is known that Eq. (1) is best suited for rigid and uniform thin layers and the approximation underestimates the mass and thickness of viscoelastic materials (Höök et al., 2001). Therefore the results obtained from Eq. (1) were compared with calculations based on the equation derived (Naderi & Claesson, 2006) from Johannsmann's model (Johannsmann, Mathauer, Wegner, & Knoll, 1992),

$$\hat{m}* = m^0\left(1 + \hat{J}(f)\frac{\rho f^2 d^2}{3}\right) \quad (2)$$

where $\hat{m}*$ is the equivalent mass, ρ is the density of the fluid, d is the thickness of the film, $\hat{J}(f)$ the complex shear assumed independent of frequency and m^0 is the true sensed mass. The latter is obtained from the intercept of a plot taking the equivalent mass as the function of frequency squared.

The viscoelastic properties of the adsorbed layers can be estimated by periodically stopping the oscillation of the quartz crystal. Damping of the oscillation due to frictional losses can be monitored. This is usually presented as the dissipation factor, defined as,

$$D = \frac{E_{\mathrm{diss}}}{2\pi E_{\mathrm{stored}}}, \quad (3)$$

where E_{diss} is the dissipated energy during one oscillation and E_{stored} is the total energy stored in the oscillation system. Viscoelastic materials have faster damping, which corresponds to higher changes in the D-value.

The adsorbed layers, without addition of background electrolyte, were also analysed using the Voigt-based model provided by commercial Q-Tools data analysis program (Q-Sense, Västra Frölunda, Sweden), based on the model by Voinova et al. (1999). Calculations were done using the parameters defined by Tammelin, Paananen, & Österberg (2009), who studied the interactions between hemicellulose and regenerated cellulose films. The fitting parameter was $1200\,\mathrm{kg/m^3}$ for the adsorbed layer density and 3rd, 5th and 7th overtones (15, 25 and 35 MHz) were modeled together to obtain comparable results. However, as the fitting includes rather crude assumptions of different layer density properties, the results should not be considered absolute values, but used for general comparison. Experiments were performed with a controlled flow rate of 100 μl/min of the diluted hemicellulose samples through the sensor chambers. The temperature was maintained at 24 °C. Measurements were repeated up to 5 times, with a minimum of two representative individual experiments on separately prepared systems.

2.4. Surface plasmon resonance (SPR)

To estimate the effect on the sensed mass in QCM-D experiments of water retained by the adsorption system, selected hemicelluloses were also characterized with surface plasmon resonance (SPR). The method is based on work by Kretschmann (1971) and is able to estimate adsorption without being affected by co-adsorbed water. More information on the theoretical basis of the technique can be found in review articles e.g. (Green et al., 2000; Liedberg, Nylander, & Lundström, 1995). To prepare films of cellulose nanofibrils on SPR chips, a procedure described in detail by Ahola, Myllytie, et al. (2008) was followed and the results were calculated using the refractive index increment determined by Hedin, Löfroth, & Nydén (2007).

Measurements were done with the Biacore 1000 instrument (GE Healthcare, Uppsala, Sweden). The same dilution concentrations as in QCM-D experiments were used, with additional degassing of water and a filtering step (0.22 μm Millipore filters GV) before injection. Also, 0.005% of surfactant P20 was added to water to ensure that clogging did not occur, but hemicelluloses were also run without it to verify that the surfactant did not alter interactions with the nanofibril films. The films were equilibrated by first flowing water over them for 2 h, after which 300 μl of polysaccharide solution was injected. The flow rate was 5 μl/min and the temperature was kept constant at 25 °C. The results were shifted to set the baseline at 0 response units prior to sample injection. With NFC films uniform thickness across the sensor surface is challenging to achieve, and the starting level varied within both measurement channels and sensors. Each sample was measured twice to verify reproducibility.

3. Results

3.1. Interaction of spruce galactoglucomannan and xyloglucan with hardwood cellulose nanofibril substrates

The bio-inspired interactions were studied with biomaterials with large-scale production and application possibilities. The association of several structurally different hemicelluloses with cellulosic nanofibril substrates was compared. The NFC substrate was furthermore representative of the native kraft pulp fibre chemistry and morphology thus improving the basic knowledge of fibre-hemicellulose interactions. Adsorption was studied in the aqueous state using QCM-D. Fig. 2 shows the kinetics of hemicellulose attachment on the nanofibrillar film coated quartz sensor during the first hour of adsorption. Estimations of the aqueous bound mass, Δm, (calculated by Eqs. (1) and (2)), and changes in energy dissipation, ΔD, upon hemicellulose adsorption (Eq. (3)) are shown in Fig. 2a and b, respectively. Spruce galactoglucomannan (GGM) adsorbed on cellulose substrate well and irreversibly, although the adsorbed amount was less than that observed for xyloglucan (XG). However, the corresponding ΔD-values were also lower with GGM compared to XG, indicating a less viscoelastic structure. This was also seen from the more overlapping estimations for GGM Δm values when comparing the viscoeleastic Johannsmann estimation (Eq. (2)) to the basic Sauerbrey equation (Eq. (1)). For XG, the viscoelastic estimation gave higher adsorbed mass.

3.2. Interaction of cereal arabinoxylans with hardwood cellulose nanofibril substrates

Corresponding QCM-D results for the different cereal arabinoxylans (AX) are presented in Fig. 3. The properties of the adsorbed layer on hardwood cellulose nanofibril films were rather divergent. All cereal AX had a lower increase in adsorbed mass compared to XG. However, rye-and wheat AX (RAX and WAX, respectively) increased the adsorbed mass more than GGM, whereas oat spelt arabinoxylan (OAX) had lower Δm-value. Enzymatically hydrolyzed $\mathrm{WAX_e}$ showed weak attachment and barely adsorbed. The simultaneously detected ΔD-values (Fig. 3b), followed the same relative order as the detected increase in mass. Compared to XG (and GGM), all native AX had higher ΔD-values. RAX had the highest ΔD-value, followed by WAX and OAX with values of

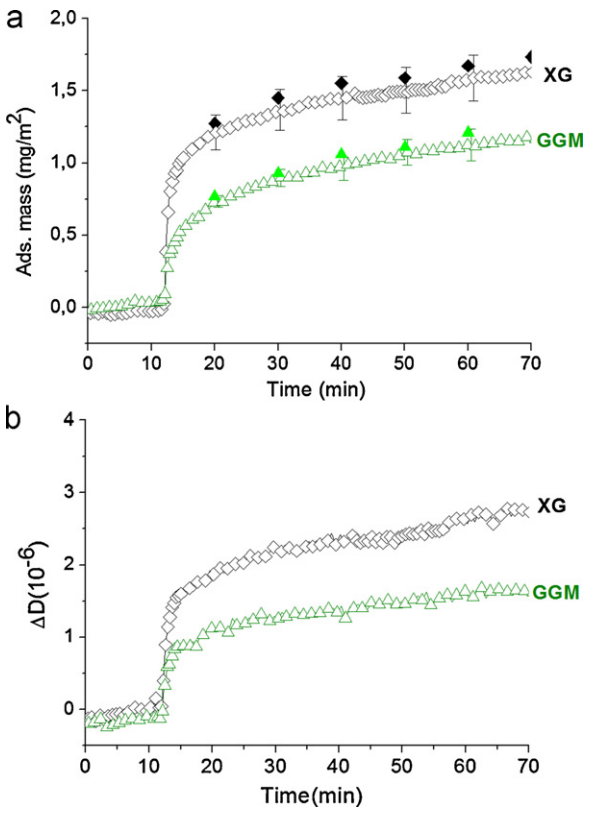

Fig. 2. Comparison of sensed mass values (a) and corresponding energy dissipation values (b) of XG (◊) and GGM (△) adsorption on hardwood nanocellulose film as the function of time. The open symbols represent the values calculated with Sauerbrey equation (Eq. (1)) and the closed symbols the values calculated with the viscoelastic Johannsmann model (Eq. (2)). Error bars show standard deviation between parallel measurements (representative adsorption is shown).

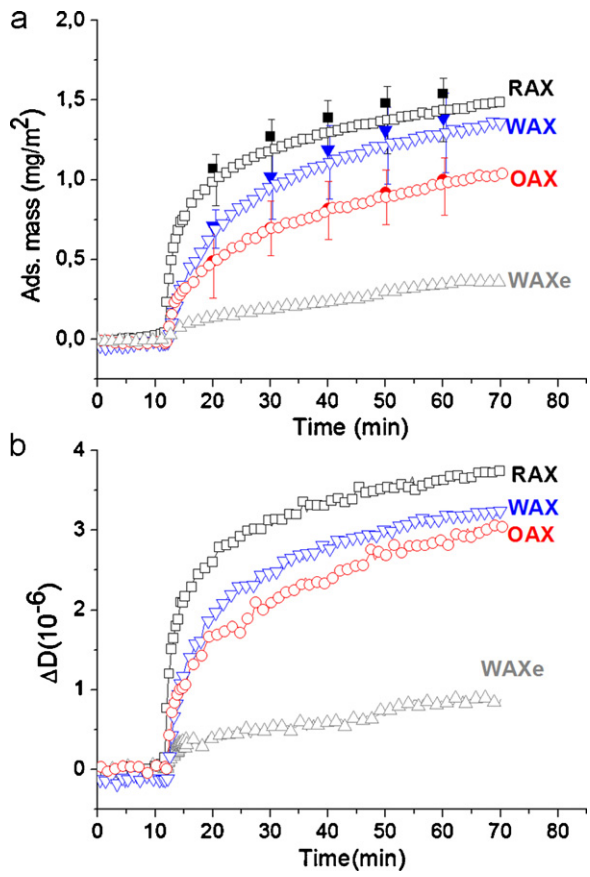

Fig. 3. Comparison of sensed mass values (a) and corresponding energy dissipation values (b) of different and modified cereal arabinoxylan adsorption on hardwood nanocellulose film as the function of time. The cereal AX compared were RAX (□), WAX (▽), OAX (○) and enzymatically modified WAX_e (△). The open symbols represent the values calculated with Sauerbrey equation (Eq. (1)) and the closed symbols the values calculated with the viscoelastic Johannsmann model (Eq. (2)). Error bars show standard deviation between parallel measurements (representative adsorption is shown).

similar magnitude. OAX had the highest relative difference between mass and energy dissipation increase, with low Δm-value but yet rather high ΔD-value. The very low increase in WAX_e ΔD-values was in good agreement with the equally low Δm-values. However, compared to XG (and GGM), all native AX had higher ΔD-values. This implies differences in the adsorbed layer conformation and viscoelastic properties, namely formation of a looser bound aqueous layer on the cellulose nanofibril substrate. Also it indicates that AXs have a lower affinity to the hardwood cellulose surface than XG.

3.3. *Effect of rinsing and comparison of bound water in adsorbed layer*

The comparison of the adsorbed amounts of the different hemicelluloses on NFC films is shown in Table 2. The results were calculated by Eq. (2) as average values from several experiments, at the point where adsorption had levelled off (2–3 h). After adsorption the system was rinsed with water to evaluate possible detachment of polysaccharides. XG had the strongest affinity towards nanofibrillar cellulose, evident from the highest increase in mass, accompanied with rather low increase in ΔD and almost irreversible attachment. WAX_e also had equally irreversible attachment, but the total adsorbed amount was very low. RAX, WAX and GGM had very similar values for the mass of the adsorbed aqueous hemicellulose before rinsing. However, rinsing removed GGM less than RAX and WAX, suggesting a stronger attachment of GGM on NFC substrate. Curiously, the latter two had an equal desorption percentage. OAX had the highest relative detachment: about 20% of the adsorbed mass was removed upon rinsing indicating that a significant part of adsorption on NFC was reversible. To estimate the amount of water bound in the adsorbed polysaccharide layers, the experiments were repeated with Surface Plasmon Resonance (SPR) for XG, GGM and WAX. These three hemicelluloses were chosen due to their different chemical structures and because QCM-D indicated clear differences in their adsorbed layer properties. Results are combined in Table 2. GGM had the highest adsorbed

Table 2
Adsorbed amount of hemicelluloses on NFC film by QCM-D and SPR and amount of coupled water.

Sample	Ads. amount QCM-D[a] [mg/m^2]	detached in rinsing[b] [%]	Ads. amount SPR[c] [mg/m^2]	water content[d] [%]
XG	2.1	1	0.5	76
GGM	1.5	9	0.6	65
OAX	1.2	21	–	–
RAX	1.5	13	–	–
WAX	1.7	13	0.4	76
WAX_e	0.5	1	–	–

[a] Calculated using the Johannsmann approximation (Eq. (2)) and reported from the end of experiments.
[b] Calculated by comparing the values before and after rinsing step.
[c] Approximation calculated using the equation and parameters of Hedin et al. (2007).
[d] Calculated by comparing the estimations from SPR and QCM-D.

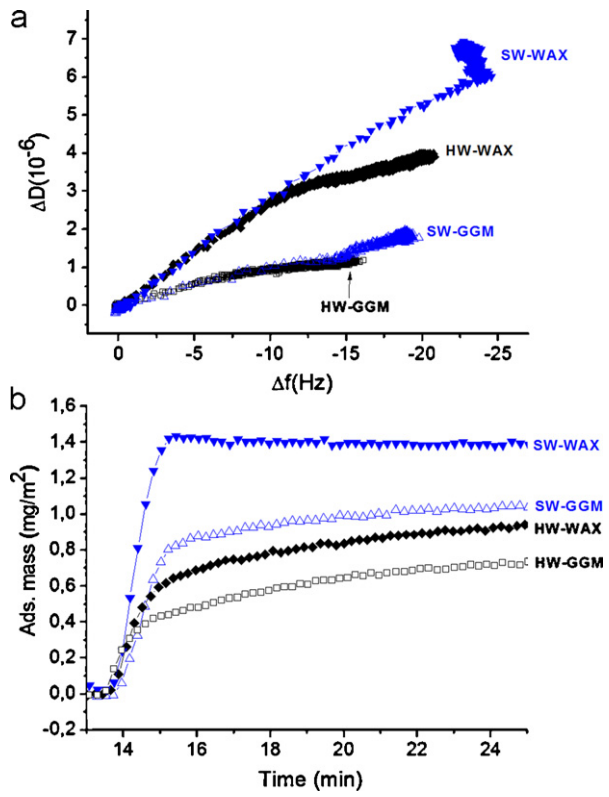

Fig. 4. Comparison of hemicellulose adsorption on nanofibril cellulose films prepared either from hard- (HW) or soft-wood (SW). The change in dissipation (D) is shown as the function of the change in frequency measured at the third overtone of the 5 MHz fundamental frequency (a). The adsorption kinetics on HW and SW films is compared by plotting the sensed mass (calculated by Eq. (1)) during the first 12 min of hemicellulose adsorption on the surfaces (b).

mass using SPR, followed by XG and WAX. By comparing the QCM-D sensed mass the water content of the adsorbed layers was estimated. As expected, the relative amount of coupled water was in all cases high (about 65–75%). However, GGM layer contained somewhat less water than XG and WAX.

The adsorbed amounts observed for hemicelluloses on NFC substrate are on the same level as adsorption of cationic polymers on cellulose. For comparison, it can be noted that e.g. cationic polyacrylamide, a synthetic polymer typically used in papermaking as retention aid or strength additive, adsorbs around 1–4 mg/m^2 on cellulose substrates depending on charge and ionic strength in the solution (Saarinen, Österberg, & Laine, 2009).

3.4. Comparison of interactions with hardwood and softwood nanofibrillar substrates

The comparisons above of the interactions of hardwood cellulose nanofibrils with different hemicelluloses confirm that the chemical structure clearly affects the properties of the adsorbed hemicellulose layer. Next, adsorption of xylan (WAX) and mannan (GGM) was studied both on hardwood and softwood NFC to investigate if the chemical composition of NFC, i.e. difference in hemicellulose content and composition, affects the adsorption. According to the chemical analysis, hardwood NFC contains 26% of xylan and <2% glucomannan, and softwood NFC contains 10% arabinoxylan and 8% galactoglucomannan. QCM-D-monitoring of the adsorbed amount and of the viscoelastic properties of WAX and GGM on hardwood and softwood nanofibrils substrates are shown in Fig. 4a. The change in energy dissipation is plotted against the change in frequency, and Fig. 4b shows the corresponding kinetic development for the adsorption estimated by Eq. (1) in the beginning of the experiment. The slope of the ΔD vs Δf plot correlates with the rigidity of the adsorbed layer. The lower the slope, the more rigid the layer is. Clearly the structure of hemicellulose influenced the adsorption properties more than the source and thus composition of nanofibril film. GGM especially had rather similar low ΔD vs Δf slopes with both hardwood and softwood nanofibrils, indicative of the high affinity of the polysaccharide for the cellulose substrate. With WAX, the layers were more loose and viscoelastic regardless of the nanofibril composition. However, the WAX layer structure on softwood fibrils was even more extended and included a fast initial adsorption compared to other combinations, levelling off within minutes (Fig. 4b).

The results were also fitted using the Voigt-model to estimate viscoelastic properties. The results in Fig. 5 depict the relative increase in hydrodynamic thickness (h_f) as a function of time with the systems studied. WAX-softwood fibrils had the highest h_f value before rinsing, in good agreement with the very high ΔD values. Rather surprising is the high hydrodynamic thickness of GGM attached to the hardwood fibrils, which was not evident from the gentle ΔD vs Δf curve. Furthermore, it was even higher than the corresponding value for the WAX layer on hardwood fibrils although, upon rinsing, the values were very close with both WAX and GGM-hardwood combinations. Only GGM adsorbed on softwood nanofibrils had a notably lower hydrodynamic thickness, both before and after rinsing.

3.5. Morphology of nanofibrillar substrates

The morphology of the hardwood and softwood fibril substrates was compared with AFM-imaging (Fig. 6). Both fibrils looked similar, covering the substrate completely and having a similar root mean square (RMS) roughness values of about 3.9 nm. The height-profiles plotted from the middle of the image suggest somewhat more aggregated fibril structures for the softwood fibrils, probably from the lower degree of mechanical disintegration (passes through fluidizator). Nevertheless, the films were so similar that it can be concluded that differences in morphology are not responsible for the differences seen in adsorption. Therefore the differences in hemicellulose adsorption shown in Figs. 3–5 more likely originate from the chemical composition of the cellulose nanofibrils.

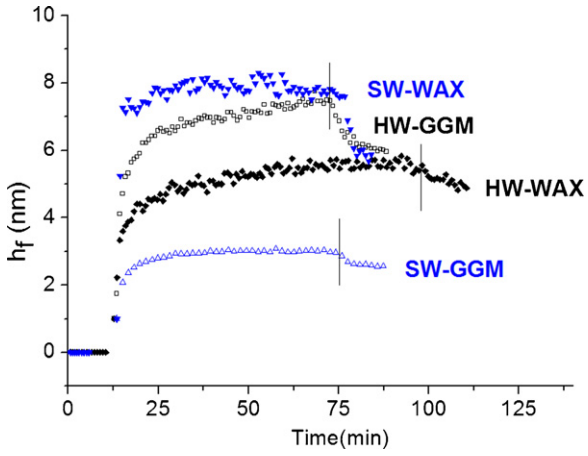

Fig. 5. The hydrodynamic thickness of the adsorbed hemicellulose layers on soft and hardwood cellulose nanofibril films as the function of time calculated from Voigt-based modelling. The bars represent the rinsing with MilliQ-water.

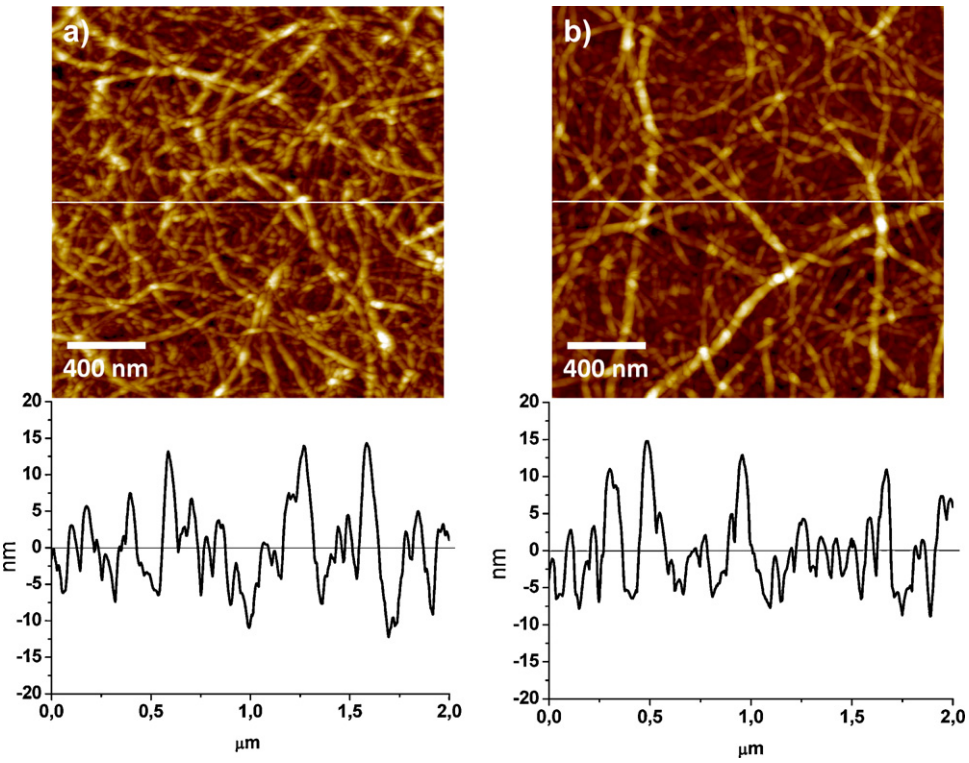

Fig. 6. 2 μm × 2 μm AFM height images of dried hardwood (a) and softwood (b) nanofibrillar model films. The height scale is 35 nm in all images and the corresponding height profile from the middle of the image are shown in graphs below. The calculated root mean square roughness (RMS) values are for (a) 3.92 nm and (b) 3.86 nm.

4. Discussion

4.1. Interactions of different hemicelluloses with hardwood NFC substrates

The hemicelluloses studied adsorbed onto NFC substrates due to the inherent interactions between hemicelluloses and cellulose fibrils, but the adsorbed layer had different properties according to the hemicellulose structure. The adsorption was characteristic of the role of hemicellulose in cell wall. XG, as the natural crosslinking component, attached to cellulose well and irreversibly, but maintained its flexibility, as seen from the relatively high ΔD-values (Fig. 2). On the other hand, GGM adsorbed in a more rigid conformation, which corresponds well to previous findings by NMR-analysis (Newman & Hemmingson, 1998; Whitney et al., 1998). The lower water content of the GGM adsorbed layer (Table 2) further supports tight association of GGM. Of course, the vast difference in molecular weights, 20 kDa (GGM) vs. 470 kDa (XG) can partly be responsible for the higher amounts of XG adsorbed. Attachment of polysaccharides to various cellulose surfaces has been noticed to increase as the function of M_w (Hayashi, Ogawa, & Mitsuishi, 1994; Kabel, van den Borne, Vincken, Voragen, & Schols, 2007; Suurnäkki, Oksanen, Kettunen, & Buchert, 2003; Vincken, de Keizer, Beldman, & Voragen, 1995), however; the extent of the side-group substitution of galactomannans affects the adsorbed amount more than just M_w. This has previously been observed using both softwood kraft pulps as substrates (Hannuksela, Tenkanen, & Holmbom, 2002) and on similar hardwood nanofibril films as in this study (Eronen, Junka, unpublished results). Previous adsorption studies with XG (Ahola, Myllytie, et al., 2008) and GGM (Tammelin et al., 2009) but with different cellulose surfaces gave equivalent results, if the influence of pH and ionic strength are taken into account. At higher pH, dissociation of the adjoined 4-O-methyl-α-D-glucuronic acid residues present in the hemicelluloses in kraft pulps promotes swelling of the film via increased electrostatic repulsion between charged cellulose segments (Donnan & Harris, 1911; Katz, Beatson, & Scallan, 1984; Lindström, 1989). Even with planar confined nanofibril substrates, this causes swelling and thus more extended conformation (Ahola, Salmi, et al., 2008), affecting the available surface area and adsorption sites.

Cereal AX have higher M_w and have a more substituted xylose backbone compared to hardwood xylans (Sjöström, 1993; Sun, Sun, & Tomkinson, 2004). The unsubstituted xylose backbone has an increased tendency to self-associate (Kabel et al., 2007; Köhnke, Pujolras, Roubroeks, & Gatenholm, 2008), which reduces solubility but also increases the amount adsorbed onto aggregated structures, as detected by AFM microscopy (Linder et al., 2003; Tammelin et al., 2009). The highly substituted cereal AXs do not extensively self-associate in solution and, upon attachment to cellulose, they may adopt an extended conformation containing loops and tails. These can entrap other AX molecules that would not otherwise be able to directly attach to the cellulose fibril surface (Kabel et al., 2007). The extension of loops also becomes more pronounced as the M_w increases. The markedly lower attachment of the enzymatically modified WAX_e sample, which is significantly reduced in M_w compared to WAX (Table 1), is in good agreement with these conclusions. Indeed, the action of xylanases is generally restricted by L-arabinofuranosyl side groups and thus enzymatic hydrolysis is expected to first proceed on the least substituted regions of the xylan backbone. The same regions of the xylan chain may be those responsible of interactions with NFC. RAX and WAX have very similar arabinose to xylose ratio (Table 1) but their substitution pattern of the arabinose side groups differs (Izydorczyk & Biliaderis, 1995). RAX contains higher amount of $(1 \rightarrow 3)$-monosubstituted and correspondingly lower amount of $(1 \rightarrow 2)(1 \rightarrow 3)$-disubstituted xylopyranosyl residues compared to WAX, which consequently leads to somewhat stiffer and extended conformation in aqueous solutions (Pitkänen et al., 2009). This

could be the reason that RAX adsorbed in a slightly more extended conformation compared to WAX (Fig. 3a and b). However, the differences between RAX and WAX were minor, especially when the polydisperse nature of hemicelluloses in solution is considered. Their amounts after rinsing were also equal.

In comparison, OAX with a lower M_w and the more linear structure similar to that of xylans present in wood (Kabelet al., 2007; Puls, Schröder, Stein, Janzon, & Saake, 2005), behaved differently. The QCM-D results support the formation of a more aggregated AX layer from the more linear structure and reduced solubility. On the other hand, visual characterization of the dried NFC substrates after experiments did not show any substantial aggregates, perhaps because they were removed by rinsing before AFM measurements. It is possible that the attached OAX was partly precipitated on top of the NFC substrates, not adsorbed and thus easily removed during rinsing. Since the hardwood NFC gel studied contains about 26% xylan, the xylan–xylan interactions could also influence the attachment of the cereal AXs to the hardwood NFC fibril substrates compared to studies with hemicellulose free celluloses.

The carbohydrate composition analysed from the disintegrated fibril suspensions corresponded well to both hardwood and softwood kraft pulp inner layer composition (Dahlman et al., 2003). Mechanical treatments of the fibres release more organic substances from hardwood fibres compared to softwood fibres and also increase in the salt concentration and pulp fibre charge density enhance the release (Sjöström, Laine, & Blademo, 2000). In the same study, re-adsorption was evident only at high salt concentrations. However, Roberts and El-Karim (1983) speculated that, under mechanical shear, xylans (arabinoxylans in their case) dissolve and redistribute on the opened fibre structure (Roberts & El-Karim, 1983). Mora, Ruel, Comtat, & Joseleau (1986) visualized some alkali- and DMSO-soluble aggregates after beating suspected to originate from xylan (Mora et al., 1986); and also for softwood kraft fibres an enrichment of glucuronoxylan has been located on the outer fibre wall (Köhnke, Lund, Brelid, & Westman, 2010). Therefore, it is possible that xylan could influence the observed hemicellulose interactions so a comparison to softwood fibrils containing a lower percentage of xylan was performed.

4.2. Comparison of adsorption to hardwood and softwood nanofibrillar substrates

The carbohydrate composition of the nanofibrils affected the interactions with the hemicelluloses in a consistent manner. Both WAX and GGM had almost similar attachment to hardwood and softwood fibril films, although Voigt-modelling revealed the relative viscoelastic differences of the attached layers. In a previous comparison of GGM with different industrial pulps, the sorbed amounts on both hardwood and softwood kraft pulps were also very similar (Hannuksela, Fardim, & Holmbom, 2003). The smaller relative hydrodynamic thickness also confirms the tight association between hemicellulose and cellulose fibrils present in the native softwood (spruce) cell wall. In comparison, the hydrodynamic thickness was doubled for the GGM-hardwood combination. Galactomannan affinity to cotton cellulose has been found to be independent of the presence of xylan (Hansson, 1970) but not vice versa. The presence of galactomannan affects xylan adsorption (Hansson & Hartler, 1969). For the soluble, highly substituted and high M_w cereal AX used in this study, the amount adsorbed was not affected much by the chemical composition of the cellulose fibrils, probably because the adsorption was enhanced more by the formation of extended loops. However, the somewhat faster adsorption and looser layer of WAX with softwood fibrils indicates that hemicelluloses could influence the interactions. Hardwood glucuronoxylans do not contain the additional α-L-arabinofuranosyl substituents which are present in softwood arabinoglucuronoxylans (Sjöström, 1993). The relatively higher desorption caused by rinsing reduced the hydrodynamic thickness of WAX on softwood to the same level compared to hardwood HW-WAX and GGM combinations. This also suggested formation of some loosely bound aggregates. The quite high hydrodynamic thickness of GGM with hardwood fibrils was not expected from the similar energy dissipation values with softwood attachment. The reason could be that the relatively linear GGM is not able to attach as tightly in the absence of mannan–mannan interactions. For clarification of the role of hemicelluloses in the sorption properties of nanofibrillar substrates, more experiments should be performed with NFCs prepared from high xylan content kraft fibres. To our knowledge, this is the first study to indicate that the pulp used as raw material for NFC preparation influences also the interactions with hemicelluloses. This suggests that the different content and composition of hemicelluloses in pulp is preserved in the NFC substrates and could possibly have influence also on NFC applications.

5. Conclusions

Interactions between mechanically disintegrated cellulose nanofibrils and well-characterized hemicelluloses were studied. The nanofibrils also contain hemicelluloses, and the proportion and composition depends on the raw material used. Results verify the adsorption of similar (1 → 4)-β-D-linked cellulose and hemicelluloses, with different backbone constituents detected previously on different cellulose substrates. The properties of adsorbed layers of model hemicelluloses can be related to their general role in native wood cell-walls. GGM had a tighter association compared to cereal-AXs, but XG had the highest and most irreversible attachment to hardwood nanofibrils. A comparison of softwood and hardwood fibrils with similar morphology but different hemicelluloses composition did not reveal major differences in the interactions. However, viscoelastic modelling of the QCM-D results suggested that the native softwood hemicellulose (GGM) and nanosized fibrils from softwood attached in closer association compared to hardwood fibrils. This could possibly be influenced by the tighter mannan–mannan interactions. Other reason could be the influence of the higher hemicellulose content in hardwood fibres. The fact that hemicelluloses readily adsorb on cellulose fibrils offers interesting possibilities for more functional modifications to create new, efficient renewable materials.

Acknowledgements

This work was financed by funding from the Finnish Funding Agency for Technology and Innovation (TEKES), industrial partners within Naseva-project, and the University of Helsinki research funds. The Finnish centre for Nanocellulose technologies is acknowledged for providing the NFC samples and Prof. Stefan Willför from the Åbo Akademi University (Finland) for GGM. M.Sc. Tuija Teerinen from VTT Biotechnology (Finland) is gratefully acknowledged for help with SPR-experiments and Dr. Tarja Tamminen and Dr. Satu Vuorela (VTT) for the carbohydrate composition analysis of NFC samples. Dr. Kirsi Parikka (University of Helsinki) is thanked for drawing the polysaccharide structures (Fig. 1) and Dr. Joseph Campbell (Aalto University) for the linguistic revision of the manuscript.

References

Ahola, S., Myllytie, P., Österberg, M., Teerinen, T., & Laine, J. (2008). Effect of polymer adsorption on cellulose nanofibril water binding capacity and aggregation. *BioResources*, *3*(4), 1315–1328.

Ahola, S., Salmi, J., Johansson, L. S., Laine, J., & Österberg, M. (2008). Model films from native cellulose nanofibrils. Preparation, swelling, and surface interactions. *Biomacromolecules*, *9*(4), 1273–1282.

Almond, A., & Sheehan, J. K. (2003). Predicting the molecular shape of polysaccharides from dynamic interactions with water. *Glycobiology*, *13*(4), 255–264.
Burton, R. A., Gidley, M. J., & Fincher, G. B. (2010). Heterogeneity in the chemistry, structure and function of plant cell walls. *Nature Chemical Biology*, *6*(10), 724–732.
Dahlman, O., Jacobs, A., & Sjöberg, J. (2003). Molecular properties of hemicelluloses located in the surface and inner layers of hardwood and softwood pulps. *Cellulose*, *10*(4), 325–334.
Donnan, F., & Harris, A. (1911). The osmotic pressure and conductivity in aqueous solutions of Congo-red and reversible membrane equilibria. *Journal of The Chemical Society*, *99*, 1554–1577.
Ebringerová, A. (2005). Structural diversity and application potential of hemicelluloses. *Macromolecular Symposia*, *232*(1), 1–12.
Eichhorn, S., Dufresne, A., Aranguren, M., Marcovich, N., Capadona, J., Rowan, S., et al. (2010). Review: Current international research into cellulose nanofibres and nanocomposites. *Journal of Materials Science*, *45*(1), 1–33.
Fengel, D., & Wegener, G. (1984). *Wood: Chemistry, ultrastructure, reactions*. Berlin, Fed.Rep. Ger.: Walter de Gruyter.
Green, R. J., Frazier, R. A., Shakesheff, K. M., Davies, M. C., Roberts, C. J., & Tendler, S. J. B. (2000). Surface plasmon resonance analysis of dynamic biological interactions with biomaterials. *Biomaterials*, *21*(18), 1823–1835.
Hannuksela, T., Fardim, P., & Holmbom, B. (2003). Sorption of spruce O-acetylated galactoglucomannans onto different pulp fibres. *Cellulose*, *10*(4), 317–324.
Hannuksela, T., Tenkanen, M., & Holmbom, B. (2002). Sorption of dissolved galactoglucomannans and galactomannans to bleached kraft pulp. *Cellulose*, *9*(3), 251–261.
Hansen, N. M. L., & Plackett, D. (2008). Sustainable films and coatings from hemicelluloses: A review. *Biomacromolecules*, *9*(6), 1493–1505.
Hansson, J.-Å. (1970). Sorption of hemicelluloses on cellulose fibres, Pt. 2. Sorption of glucomannan. *Holzforschung*, *24*(3), 77–83.
Hansson, J.-Å., & Hartler, N. (1969). Sorption of hemicelluloses on cellulose fibres. Part 1. Sorption of xylans. *Svensk Papperstidning*, *72*(17), 521–530.
Hayashi, T., Ogawa, K., & Mitsuishi, Y. (1994). Characterization of the adsorption of xyloglucan to cellulose. *Plant and Cell Physiology*, *35*(8), 1199–1205.
Hedin, J., Löfroth, J.-E., & Nydén, M. (2007). Adsorption behavior and cross-linking of EHEC and HM-EHEC at hydrophilic and hydrophobic modified surfaces monitored by SPR and QCM-D. *Langmuir*, *23*(11), 6148–6155.
Höije, A., Sternemalm, E., Heikkinen, S., Tenkanen, M., & Gatenholm, P. (2008). Material properties of films from enzymatically tailored arabinoxylans. *Biomacromolecules*, *9*(7), 2042–2047.
Höök, F., Kasemo, B., Nylander, T., Fant, C., Sott, K., & Elwing, H. (2001). Variations in coupled water, viscoelastic properties, and film thickness of a Mefp-1 protein film during adsorption and cross-linking: A quartz crystal microbalance with dissipation monitoring, ellipsometry, and surface plasmon resonance study. *Analytical Chemistry*, *73*(24), 5796–5804.
Iwamoto, S., Abe, K., & Yano, H. (2008). The effect of hemicelluloses on wood pulp nanofibrillation and nanofiber network characteristics. *Biomacromolecules*, *9*(3), 1022–1026.
Izydorczyk, M. S., & Biliaderis, C. G. (1995). Cereal arabinoxylans: Advances in structure and physicochemical properties. *Carbohydrate Polymers*, *28*(1), 33–48.
Johannsmann, D., Mathauer, K., Wegner, G., & Knoll, W. (1992). Viscoelastic properties of thin films probed with a quartz-crystal resonator. *Physical Review B*, *46*(12), 7808–7815.
Joseleau, J. P., Comtat, J., & Ruel, K. (1992). Chemical structure of xylans and their interaction in the plant cell walls. In J. Visser, G. Beldman, M. A. Kusters-van Someron, & A. G. J. Voragen (Eds.), *Progress in biotechnology* (pp. 1–15). Amsterdam: Elsevier.
Kabel, M. A., van den Borne, H., Vincken, J.-P., Voragen, A. G. J., & Schols, H. A. (2007). Structural differences of xylans affect their interaction with cellulose. *Carbohydrate Polymers*, *69*(1), 94–105.
Katz, S., Beatson, R. P., & Scallan, A. M. (1984). The determination of strong and weak acidic groups in sulfite pulp. *Svensk Papperstidning*, *87*(6), R48–R53.
Kretschmann, E. (1971). Determination of the optical constants of metals by excitation of surface plasmons. *Zeitschrift für Physik*, *241*(4), 313–324.
Köhnke, T., Lund, K., Brelid, H., & Westman, G. (2010). Kraft pulp hornification: A closer look at the preventive effect gained by glucuronoxylan adsorption. *Carbohydrate Polymers*, *81*(2), 226–233.
Köhnke, T., Pujolras, C., Roubroeks, J., & Gatenholm, P. (2008). The effect of barley husk arabinoxylan adsorption on the properties of cellulose fibres. *Cellulose*, *15*(4), 537–546.
Liedberg, B., Nylander, C., & Lundström, I. (1995). Biosensing with surface plasmon resonance: How it all started. *Biosensors and Bioelectronics*, *10*(8), i–ix.
Lima, D. U., Oliveira, R. C., & Buckeridge, M. S. (2003). Seed storage hemicelluloses as wet-end additives in papermaking. *Carbohydrate Polymers*, *52*(4), 367–373.
Linder, Å., Bergman, R., Bodin, A., & Gatenholm, P. (2003). Mechanism of assembly of xylan onto cellulose surfaces. *Langmuir*, *19*(12), 5072–5077.
Lindström, T. (1989). Some fundamental chemical aspects on paper forming. In C. F. Baker, & V. W. Punton (Eds.), *Fundamentals of papermaking* (pp. 311–412). London: Mech. Eng. Pub. Ltd.
Mikkonen, K., Mathew, A., Pirkkalainen, K., Serimaa, R., Xu, C., Willför, S., et al. (2010). Glucomannan composite films with cellulose nanowhiskers. *Cellulose*, *17*(1), 69–81.
Mikkonen, K. S., Heikkinen, S., Soovre, A., Peura, M., Serimaa, R., Talja, R. A., et al. (2009). Films from oat spelt arabinoxylan plasticized with glycerol and sorbitol. *Journal of Applied Polymer Science*, *114*(1), 457–466.
Mora, F., Ruel, K., Comtat, J., & Joseleau, J. P. (1986). Aspect of native and redeposited xylans at the surface of cellulose microfibrils. *Holzforschung*, *40*(2), 85–91.
Naderi, A., & Claesson, P. M. (2006). Adsorption properties of polyelectrolyte-surfactant complexes on hydrophobic surfaces studied by QCM-D. *Langmuir*, *22*(18), 7639–7645.
Newman, R. H., & Hemmingson, J. A. (1998). Interactions between locust bean gum and cellulose characterized by13C NMR spectroscopy. *Carbohydrate Polymers*, *36*(2–3), 167–172.
Paananen, A., Österberg, M., Rutland, M. W., Tammelin, T., Saarinen, T., Tappura, K., et al. (2004). Interactions between cellulose and xylan: An atomic force microscope and quartz crystal microbalance study. In P. Gatenholm, & M. Tenkanen (Eds.), *Hemicelluloses: Science and technology* (pp. 269–290). Washington, DC: American Chemical Society.
Parikka, K., Leppänen, A.-S., Pitkänen, L., Reunanen, M., Willför, S., & Tenkanen, M. (2010). Oxidation of polysaccharides by galactose oxidase. *Journal of Agricultural and Food Chemistry*, *58*(1), 262–271.
Picout, D. R., Ross-Murphy, S. B., Errington, N., & Harding, S. E. (2003). Pressure cell assisted solubilization of xyloglucans: Tamarind seed polysaccharide and detarium gum. *Biomacromolecules*, *4*(3), 799–807.
Pitkänen, L., Virkki, L., Tenkanen, M., & Tuomainen, P. (2009). Comprehensive multidetector HPSEC Study on solution properties of cereal arabinoxylans in aqueous and DMSO solutions. *Biomacromolecules*, *10*(7), 1962–1969.
Puls, J., Schröder, N., Stein, A., Janzon, R., & Saake, B. (2005). Xylans from oat spelts and birch kraft pulp. *Macromolecular Symposia*, *232*(1), 85–92.
Pääkkö, M., Ankerfors, M., Kosonen, H., Nykänen, A., Ahola, S., Österberg, M., et al. (2007). Enzymatic hydrolysis combined with mechanical shearing and high-pressure homogenization for nanoscale cellulose fibrils and strong gels. *Biomacromolecules*, *8*(6), 1934–1941.
Roberts, J. C., & El-Karim, S. A. (1983). The behavior of surface adsorbed xylans during the beating of a bleached kraft pine pulp. *Cellulose Chemistry and Technology*, *17*(4), 379–386.
Rodahl, M., Höök, F., Krozer, A., Brzezinski, P., & Kasemo, B. (1995). Quartz crystal microbalance setup for frequency and Q-factor measurements in gaseous and liquid environments. *Review of Scientific Instruments*, *66*(7), 3924–3930.
Salmén, L., & Olsson, A.-M. (1998). Interaction between hemicelluloses, lignin and cellulose: Structure–property relationships. *Journal of Pulp and Paper Science*, *24*(3), 99–103.
Saarinen, T., Österberg, M., & Laine, J. (2009). Properties of cationic polyelectrolyte layers adsorbed on silica and cellulose surfaces studied by QCM-D: Effect of polyelectrolyte charge density and molecular weight. *Journal of Dispersion Science and Technology*, *30*(6), 969–979.
Scheller, H. V., & Ulvskov, P. (2010). Hemicelluloses. *Annual Review of Plant Biology*, *61*(1), 263–289.
Siró, I., & Plackett, D. (2010). Microfibrillated cellulose and new nanocomposite materials: A review. *Cellulose*, *17*(3), 459–494.
Sjöström, E. (1993). *Wood chemistry: Fundamentals and applications* (2nd rev. ed). San Diego (CA): Academic Press.
Sjöström, L., Laine, J., & Blademo, Å. (2000). Release of organic substances from bleached sulphate pulps during slushing and refining. *Nordic Pulp and Paper Research Journal*, *15*(5), 469–475.
Sun, R., Sun, X. F., & Tomkinson, J. (2004). Hemicelluloses and their derivatives. In P. Gatenholm, & M. Tenkanen (Eds.), *Hemicelluloses: Science and technology* (pp. 2–22). Washington, DC: American Chemical Society.
Sundberg, A., Sundberg, K., Lillandt, C., & Holmbom, B. (1996). Determination of hemicelluloses and pectins in wood and pulp fibres by acid methanolysis and gas chromatography. *Nordic Pulp & Paper Research Journal*, *11*(4), 216–219.
Suurnäkki, A., Oksanen, A. T., Kettunen, H., & Buchert, J. (2003). The effect of mannan on physical properties of EGF bleached softwood kraft fibre handsheets. *Nordic Pulp and Paper Research Journal*, *18*(4), 429–435.
Tammelin, T., Paananen, A., & Österberg, M. (2009). Hemicelluloses at interfaces: Some aspects of the interactions. In L. A. Lucia, & O. J. Rojas (Eds.), *The nanoscience and technology of renewable biomaterials* (pp. 149–171). Chichester: Wiley-Blackwell Publishing Ltd.
Tenkanen, M., Gellerstedt, G., Vuorinen, T., Teleman, A., Perttula, M., Li, J., et al. (1999). Determination of hexenuronic acid in softwood kraft pulps by three different methods. *Journal of Pulp and Paper Science*, *25*(9), 305–311.
Westbye, P., Svanberg, C., & Gatenholm, P. (2006). The effect of molecular composition of xylan extracted from birch on its assembly onto bleached softwood kraft pulp. *Holzforschung*, *60*(2), 143–148.
Whitney, S. E. C., Brigham, J. E., Darke, A. H., Reid, J. S. G., & Gidley, M. J. (1998). Structural aspects of the interaction of mannan-based polysaccharides with bacterial cellulose. *Carbohydrate Research*, *307*(3–4), 299–309.
Willför, S., Rehn, P., Sundberg, A., Sundberg, K., & Holmbom, B. (2003). Recovery of water-soluble acetylgalactoglucomannans from mechanical pulp of spruce. *Tappi Journal*, *2*(11), 27–32.
Willför, S., Sundberg, K., Tenkanen, M., & Holmbom, B. (2008). Spruce-derived mannans: A potential raw material for hydrocolloids and novel advanced natural materials. *Carbohydrate Polymers*, *72*(2), 197–210.
Vincken, J.-P., de Keizer, A., Beldman, G., & Voragen, A. G. J. (1995). Fractionation of xyloglucan fragments and their interaction with cellulose. *Plant Physiology*, *108*(4), 1579–1585.

Virkki, L., Maina, H. N., Johansson, L., & Tenkanen, M. (2008). New enzyme-based method for analysis of water-soluble wheat arabinoxylans. *Carbohydrate Research*, *343*(3), 521–529.

Voinova, M. V., et al. (1999). Viscoelastic acoustic response of layered polymer films at fluid–solid interfaces: Continuum mechanics approach. *Physica Scripta*, *59*(5), 391–396.

Xu, C., Willför, S., Sundberg, K., Petterson, C., & Holmbom, B. (2007). Physicochemical characterization of spruce galactoglucomannan solutions: Stability, surface activity and rheology. *Cellulose Chemistry and Technology*, *41*(1), 51–62.

Yllner, S., & Enström, B. (1957). The adsorption of xylan on cellulose fibers during the sulfate cook II. *Svensk Papperstidning*, *60*, 549–554.

Zhou, Q., Rutland, M., Teeri, T., & Brumer, H. (2007). Xyloglucan in cellulose modification. *Cellulose*, *14*(6), 625–641.